



Wearables and Detection of Falls: A Comparison of Machine Learning Methods and Sensors Positioning

Arthur B. A. Pinto¹ · Gilda A. de Assis² · Luiz C. B. Torres² · Thomas Beltrame³ · Diana M. G. Domingues^{3,4}

Accepted: 18 December 2021

© The Author(s), under exclusive licence to Springer Science+Business Media, LLC, part of Springer Nature 2022

Abstract

Wearable sensors have many applications to provide assistance for older adults. We aimed to identify the best combination of machine learning algorithms and body regions to attach one wearable for real-time falls detection from a public dataset where volunteers performed daily activities and simulated falls. Accuracy and comfort of the combination of wearables and algorithms were assessed. Raw data from the accelerometer and gyroscope were used for both training and testing stages. We evaluated the confusion matrix between all wearables at each of the different body regions (Ankle, Right Pocket, Belt, Neck, and Wrist) for the following machine learning algorithms: Multilayer Perceptron (MLP), Random Forest, XGBoost, and Long Short Term Memory (LSTM) deep neural network. The accuracy was compared by ANOVA two-way repeated measures statistical test. This work has two main technical contributions. First, our results demonstrated the highest accuracy in identifying falls when the sensors were positioned on the neck or ankle. Second, when the machine learn-

Gilda A. de Assis, Luiz C. B. Torres, Thomas Beltrame and Diana M. G. Domingues have contributed equally to this work.

✉ Gilda A. de Assis
gildaass@ufop.edu.br

Arthur B. A. Pinto
arthur.bernardo@dcc.ufmg.br

Luiz C. B. Torres
luiz.torres@ufop.edu.br

Thomas Beltrame
beltramethomas@gmail.com

Diana M. G. Domingues
dgdomingues@gmail.com

¹ Departamento de Ciência da Computação, Universidade Federal de Minas Gerais, Belo Horizonte 31270-901, Brazil

² Instituto de Ciências Exatas e Aplicadas, Universidade Federal de Ouro Preto, João Monlevade 35931-008, Brazil

³ Instituto de Computação, Universidade de Campinas, Campinas 13083-852, Brazil

⁴ Laboratório de Pesquisa em Artes e Tecnociência, Universidade de Brasília, Gama 72444-240, Brazil

ing algorithms to detect fall was compared, LSTM deep neural network and Random Forest showed statistically higher accuracy than MLP and XGBoost. Besides, a comfort analysis based on the literature concluded that neck and wrist are the most comfortable regions to wear wearables.

Keywords Fall detection · Wearables · Inertial sensors · Machine learning methods

1 Introduction

Aging is a natural process of human life; it includes physical, psychological, and social changes that affect everyone in a particular way. Currently, this process affects the world population on a large scale, becoming a significant challenge to be faced in the 21st century, as this group demands special social attention. In this context, the increase in life expectancy must be accompanied by precautions regarding health, safety, and social integration. One of the factors that require such precautions comes from the fact that approximately one-third of aged people (65+ years) have experienced at least one fall event annually [1]. Falls are the leading cause of accidental injury and death among older adults, being the second leading cause of unintentional deaths worldwide [2].

The availability of low-cost sensors and their integration into ordinary consumer products constitutes an opportunity to understand and identify falls in real life setups from longitudinal data sets. Wearable sensors for real-time fall detection have many potential benefits for older users [3].

Several studies of elderly fall detection systems with wearable sensors and depth cameras have been reported in the literature [3–5]. The performance of these systems are still not satisfying as they have a high false alarms rate. Other studies report that grouping the signals of a collection of sensors could provide higher accuracy and decreasing false alarms, resulting in a fall detection system that is more robust than a system relying on one type of sensor. The combination of accelerometers and depth cameras provides a improvement when compared to the individual use of the sensors separately [6]. Recently, researches in the use of wearable cameras for the detection of falls have been reported. For instance, [5] investigated how web cameras attached to the waists of subjects can contribute to fall detection, combining the advantages of wearable and visual sensors.

From the viewpoint of processing information of the sensors, threshold-driven and data-driven algorithms are the two main approaches that have been mostly used for fall detection. Metaheuristic optimization algorithms like Particle Swarm Optimization (PSO), Genetic Algorithms (GA), and Beetle Antennae search (BAS) are threshold-driven methods. They are widely used for the optimization based problems, including training of neural networks. [7] proposed a BAS-ADAM method to improve the performance in solving the benchmark optimization problems, including the training of a single hidden layer neural network. In [8], was applied a nature-inspired metaheuristic optimizer to the financial problem of portfolio selection. [9] proposes a threshold-driven method for fall detection combining signals from gyroscope and sound sensors using a fuzzy algorithm modified by PSO processes, and [10] proposed a framework to simultaneously address the problem of tracking control and obstacle avoidance in real-time. In short, threshold-driven methods are computationally very less expensive than machine learning algorithms and are usually applied to signals from individual sensors, such as accelerometers and gyroscopes. These methods compare measured values from sensors to threshold values. Data driven approaches as machine learning methods, are more suitable for sensors fusion [3].

According to [3], in terms of the algorithms to analyze data from wearable devices, there is a significant shift to machine learning based approaches due to machine learning methods show better accuracy and they are more robust in comparison to threshold driven methods. Approaches of deep learning are gaining popularity especially for visual sensors and sensor fusion and are becoming the state-of-the-art for fall detection [3].

Authors of [3] discuss the challenges and open issues of elderly fall detection systems. According to them, the main challenges are: (i) the lack of a benchmark data set on elderly falls, (ii) real-time fall detection, (iii) management and transmission of data from multiple sensors, (iv) security and privacy concerns, (v) mobility, scalability and flexibility limitations. Taking these concerns into account, our proposal seeks to design a fall detection solution that provides greater mobility and acceptance by the elderly population.

While the fall detection on elderly are moving towards sensor fusion combined to deep learning, it is necessary to reduce technology-related concerns to increase the safety of wearable technology by older adults aging in place. For instance, [11] investigated the predictors of users' adoption of healthcare wearable devices, and reported that material, battery, and comfort are important factors in individuals' assessment of perceived benefit for healthcare wearables. Also, [12] concluded that the acceptance of technology by older adults remotely monitored is influenced by multiple factors, including safety, independence, comfort and family burden.

Thus, to design a real-time fall detection computer system, firstly, it is necessary to collect and analyze data from wearable sensors during falls and daily activities, which can be real or simulated by the volunteers. Second, the right combination between sensors and their body locations should be accounted for higher accuracy to the point of the system to be capable of distinguishing between falls and daily activities. To provide more comfort and increasing adoption of healthcare wearables by elderly, the on-body positions should represent typical locations for wearable devices such as watches and smartphones. The main contribution of this work was to establish the best combination of body positions to attach the wearable and machine learning algorithms to identify falls in real-life setups from one wearable device. The focus was not only on the data classification problem of wearable sensors but also on providing comfort and reducing the number of wearables to be used on the construction of a feasible embedded system to integrate wearable sensors and machine learning algorithms to classify falls in real-time.

2 Material and Methods

An overview of the research methodology is presented in the Fig. 1.

2.1 Up-Fall Detection Dataset

This study performed experiments using a public database for fall detection, using only the data from wearable sensors [13]. Dataset included wearable devices data from nine males and eight females (20.47 ± 1.66 years) performing eleven activities, six of them from daily activities and five from different simulated falls. Wearable sensors acquired raw data from a 3-axis accelerometer and a 3-axis gyroscope and were attached to five different human body parts: left wrist, neck, in the right pants pocket, in the middle of the waist (belt), and on the ankle, sampled at 100 Hz.

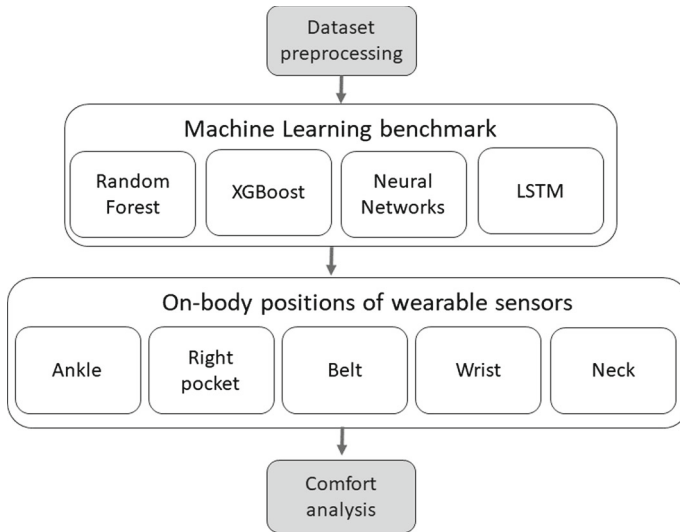


Fig. 1 Overview of the system architecture

2.2 Machine Learning Methods

Extreme Gradient Boosting (XGBoost) [14], Random Forest (RF) [15], Multi-Layer Perceptron (MLP), and long short-term memory (LSTM) deep neural network methods were chosen to implement the classifiers of activities. MLP is the most commonly used feedforward neural network [16], adjusted through the supervised training process that aims to minimize the mean quadratic error, usually, using error back-propagation method [17]. XGBoost is an open-source implementation of the framework of the Gradient Boosting decision trees [14]. RF is an ensemble method made of decision trees [15,18]. RF and XGBoost have already been applied in several classifications or regression applications, which have shown that RF and XGBoost are practical and efficient algorithms for classification problems [19]. LSTM deep neural network retain long-term information, providing the network with the ability to forecast and classify time-series [20]. An LSTM network computes a mapping from an input sequence $x = (x_1, \dots, x_T)$ to an output sequence $y = (y_1, \dots, y_T)$ by calculating the network unit activations using the following equations iteratively from $t = 1$ to T [21]:

$$i_t = \sigma(W_{ix}x_t + W_{im}m_{t-1} + W_{ic}c_{t-1} + b_i) \quad (1)$$

$$f_t = \sigma(W_{fx}x_t + W_{mf}m_{t-1} + W_{cf}c_{t-1} + b_f) \quad (2)$$

$$c_t = f_t \odot c_{t-1} + i_t \odot g(W_{cx}x_t + W_{cm}m_{t-1} + b_c) \quad (3)$$

$$o_t = \sigma(W_{ox}x_t + W_{om}m_{t-1} + W_{oc}c_t + b_o) \quad (4)$$

$$m_t = o_t \odot h(c_t) \quad (5)$$

$$y_t = W_{ym}m_t + b_y \quad (6)$$

where the W terms denote weight matrices (e.g. W_{ix} is the matrix of weights from the input gate to the input), the b terms denote bias vectors (b_i is the input gate bias vector), σ is the logistic sigmoid function, and i , f , o and c are respectively the input gate, forget gate, output gate and cell activation vectors, all of which are the same size as the cell output activation

vector m , \odot is the element-wise product of the vectors and g and h are the cell input and cell output activation functions, generally \tanh .

[22] presented a LSTM neural network for fall risk assessment. They achieved a superior classification accuracy of 92.1%, showing the potential of deep learning approaches for this kind of problem classes. They compared proposed LSTM method to three traditional machine learning methods (random forest, multilayer perceptron and support vector machine). Higher accuracy values were achieved to LSTM, random forest and multilayer perceptron. [13] performed experiments using a benchmark of machine learning models comprised of four well-known methods typically applied to fall detection (Random Forest, Support Vector Machine, Multi-Layer Perceptron and k-Nearest Neighbors). Based on these prior studies, we also have chosen LSTM, random forest and multilayer perceptron to perform the experiments. Besides these methods, we included XGBoost whereas [23] reported it has higher performance to discriminate fall from other activities.

2.3 Experimental and Evaluation Methods

The flowchart of the experiments is depicted in Fig. 2. There are two important phases shown in the flowchart: (i) Data pre-processing phase. The eleven activities were combined into three classes: Fall, Activity of Daily Living (ADL), and Picking Up an Object. All falling activities (Falling forward using hands, Falling forward using knees, Falling backward, Falling sitting in an empty chair, Falling sideward) were grouped into a “Fall” activity group. Five activities were grouped into ADL (Walking, Standing, Sitting, Jumping, Laying), and Picking Up an Object no was grouped into ADL because previous studies have reported difficulties to distinguish this activity from fall [13]. (ii) Prediction phase. In this phase, four classifiers were tested using leave-one-out cross-validation. To compare the combinations sensor body position - machine learning algorithm, we performed a statistic test of the accuracy (Fig. 3). The on-body regions of wearables were compared with data from the literature [24–26] to order from the most comfortable to the least comfortable.

2.4 Experiments

LSTM neural network parameters were chosen based in [20] while the RF, XGBoost and MLP parameters were chosen based in [13].

RF training was performed with 10 estimators and a minimal number of samples required as one. The minimum number of samples required to split an internal node was set as 2. XGBoost classifier was trained with a max depth of 10, a learning rate of 0.1, and one estimator. MLP classifier consists of an input layer, one hidden layer with 100 neurons, and an output layer. The model was trained for 200 epochs and Adam solver was used with a constant learning rate of 1×10^{-3} and an L2 penalty of 1×10^{-5} . LSTM deep neural network architecture consists of three LSTM layers (Fig. 4), each one with a hidden size of 256 hidden units and a classification layer. LSTM default parameters (bias = true, dropout = 0, bidirectional = false) were adopted and a input size of 6 was used in the first layer. The model was implemented with Pytorch¹ and trained with a maximum of 1000 epochs using the state-of-the-art Adam optimizer [27], a batch size of 512, and cross-entropy loss was used as the loss function. A cyclical learning rate varying from 5×10^{-4} to 5×10^{-6} was adopted.

¹ <https://pytorch.org/>.

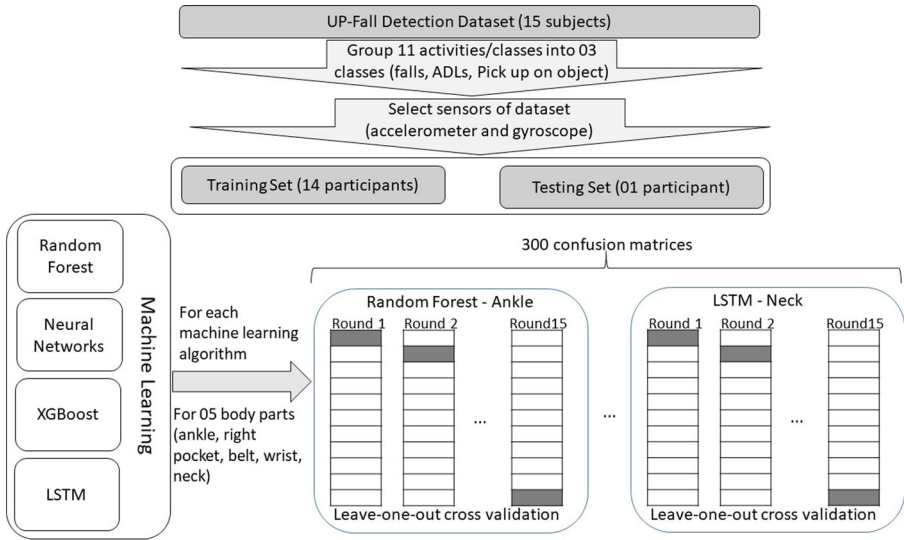


Fig. 2 The eleven activities of the Up-Fall Detection Dataset were combined into three classes: Fall, Activity of Daily Living (ADL) and Picking Up an Object. Then four classifiers, namely Random Forest, MLP, XGBoost and LSTM network were tested using leave-one-out cross-validation for all sensor regions

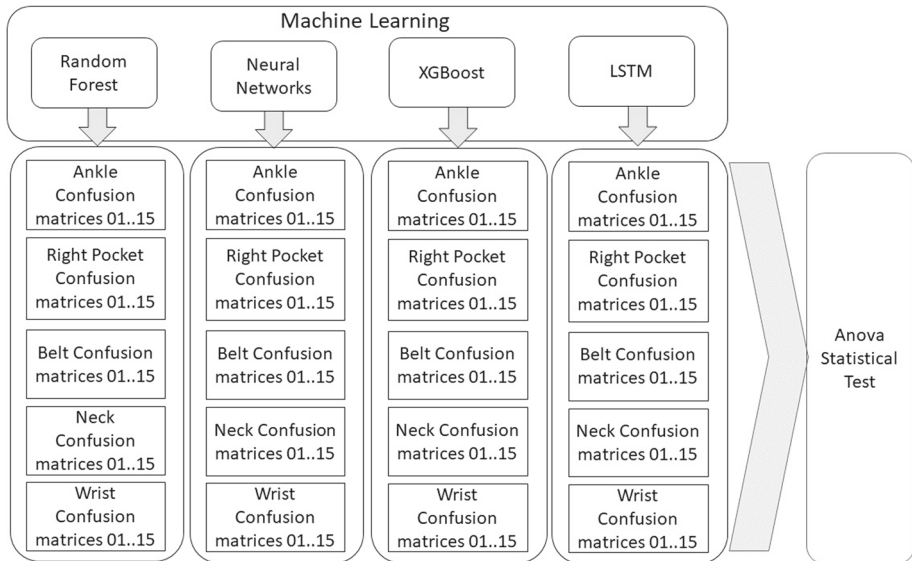


Fig. 3 Evaluation Diagram. Confusion matrices were generated for each combination of the body region (five) and the Machine learning algorithm (four) to detect fall, resulting 300 matrices. Each cell of the confusion matrices was compared by two-way repeated measures ANOVA

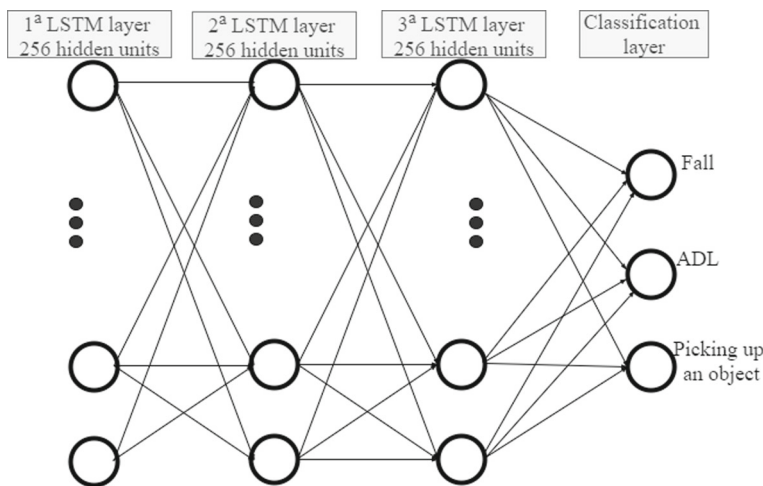


Fig. 4 LSTM architecture diagram

3 Results

3.1 Accuracy Analysis

RF, XGBoost, MLP, and LSTM were used to establish the data-driven fall detection benchmark. Data from fourteen subjects were used for training the classifier and one for validation while two subjects were discarded from the study due to technical problems during data acquisition. Data from the three axes of the accelerometer and gyroscope were used as input for the classifiers for each of the body regions (ankle, wrist, neck, the right pocket, and belt). Machine learning methods were validated by the leave-one-out cross-validation (15 rounds) for each pair (body part, machine learning algorithm). Fifteen confusion matrices were generated for each body part. Mean accuracy matrices were computed for the five body parts. Figure 5 presents mean accuracy matrices for RF, Fig. 6 for MLP, Fig. 7 for XGBoost, and Fig. 8 for LSTM method.

Table 1 shows the highest mean accuracy to classify the categories and their anatomical locations for each algorithm. The two way repeated measures analysis of variance (ANOVA) was chosen for statistical analysis. ANOVA test was performed to statistically compare the values of the accuracy of the 300 rounds performed for the four classification methods combined with the five body regions. The significance level was set as $p < 0.05$. Bonferroni t-test was applied to all pairwise multiple comparison procedures for two factors, method and body region. Tables 2 and 3 present comparisons for Method and Body Region, respectively. For falls, values of least-square means of the five regions were: Neck (0.639), ankle (0.634), right pocket (0.584), belt (0.552) and wrist (0.416). Table 4 summarizes the general performance of the methods, where the mean accuracy of the trained model is measured by the average of the correct predictions out of total samples. Pairwise multiple comparisons among regions in Table 3, regardless of the classification method, showed that the neck was statistically greater than wrist ($t < 0.001$) and belt ($t = 0.047$) while ankle was greater than wrist ($t < 0.001$) and the belt was greater than wrist ($t < 0.001$). There is no significant difference between the means of the pairs (neck, right pocket), (neck, ankle), (ankle, belt) and (ankle, right pocket). LSTM deep neural network method was statistically greater than MLP

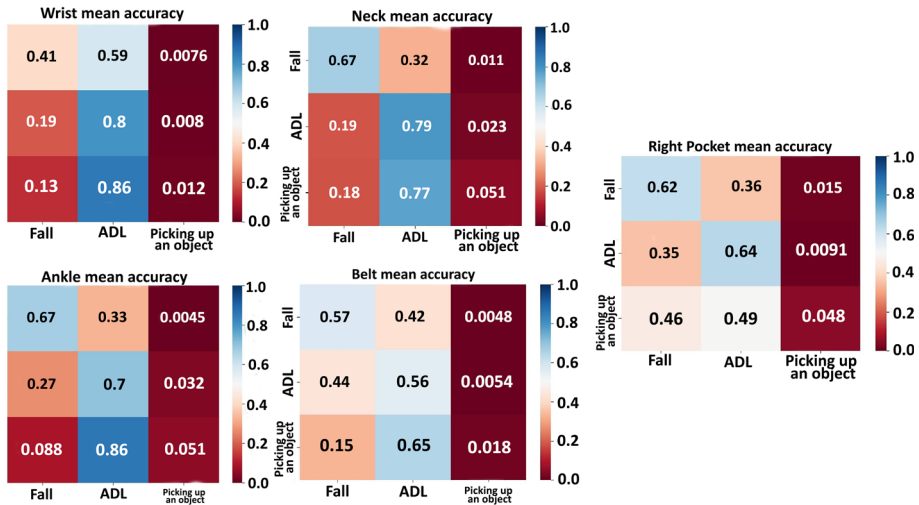


Fig. 5 RF normalized confusion matrix. The figure shows the confusion matrix for each body's region (wrist, ankle, neck, right pocket, belt) with a score of 0.0–1.0. Rows represent the real classes, and columns, the predicted class. The score shows the rate of samples assigned to a class. Consequently, the values of the diagonal elements denote the degree of correctly predicted classes by the RF algorithm

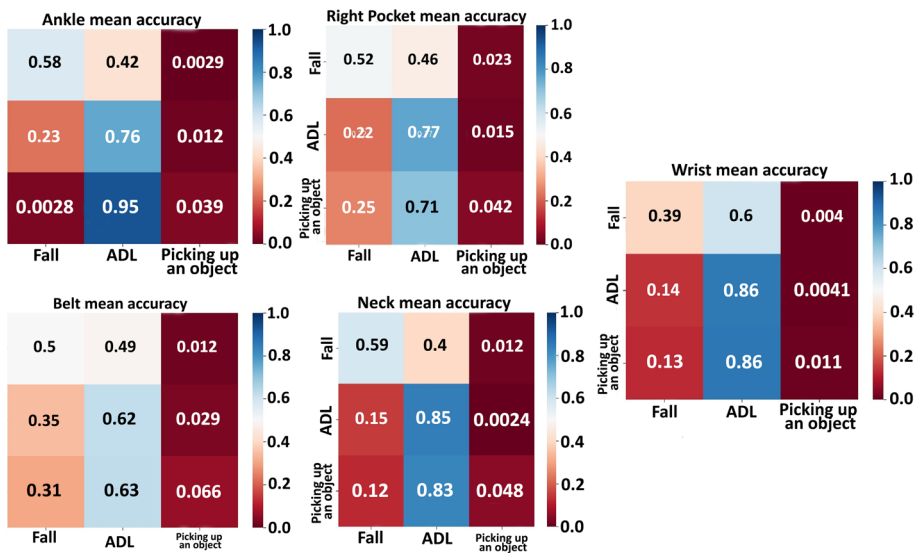


Fig. 6 MLP normalized confusion matrix. The figure shows the confusion matrix for each body's region (wrist, ankle, neck, right pocket, belt) with a score of 0.0–1.0. Rows represent the real classes, and columns, the predicted class. The score shows the rate of samples assigned to a class. Consequently, the values of the diagonal elements denote the degree of correctly predicted classes by the MLP algorithm

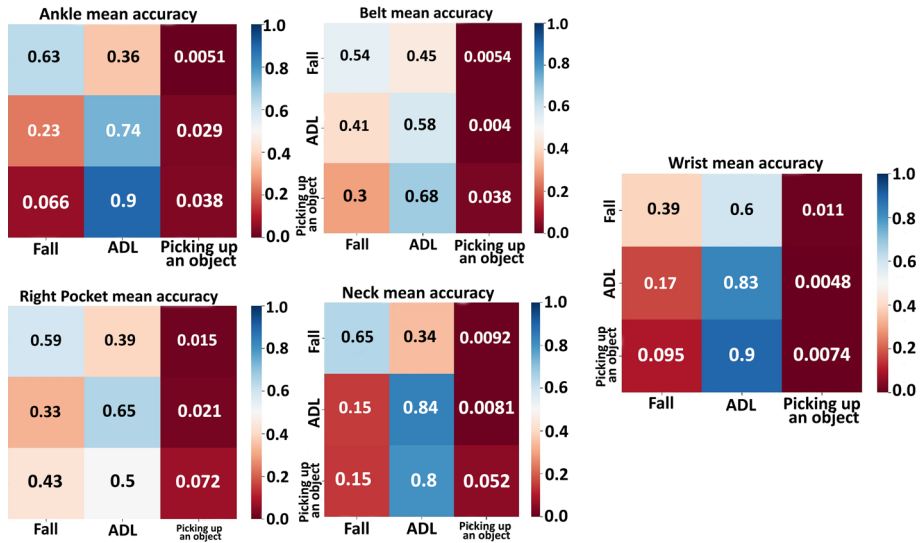


Fig. 7 XGBoost normalized confusion matrix. The figure shows the confusion matrix for each body's region (wrist, ankle, neck, right pocket, belt) with a score of 0.0–1.0. Rows represent the real classes, and columns, the predicted class. The score shows the rate of samples assigned to a class. Consequently, the values of the diagonal elements denote the degree of correctly predicted classes by the XGBoost algorithm

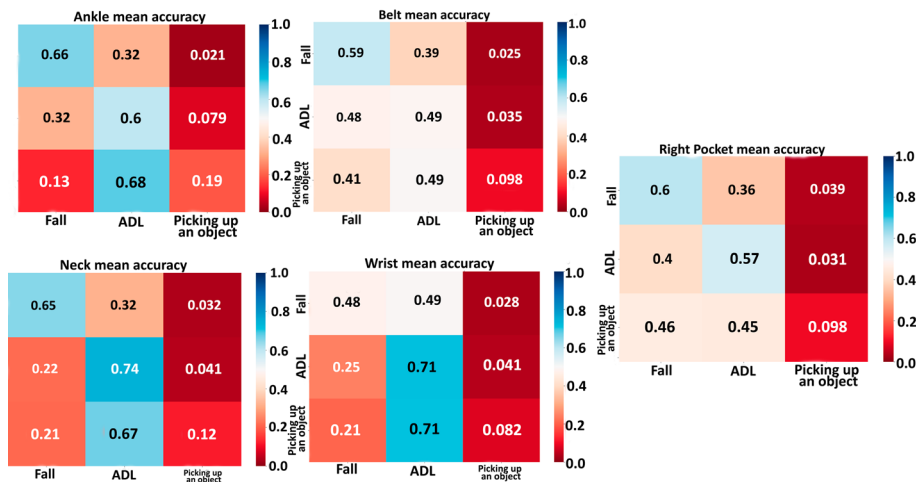


Fig. 8 LSTM normalized confusion matrix. The figure shows the confusion matrix for each body's region (wrist, ankle, neck, right pocket, belt) with a score of 0.0–1.0. Rows represent the real classes, and columns, the predicted class. The score shows the rate of samples assigned to a class. Consequently, the values of the diagonal elements denote the degree of correctly predicted classes by the LSTM algorithm

Table 1 Comparison of the highest accuracy of activities

| Activity | Region | Method | Mean Accuracy |
|----------|-------------|--------|---------------|
| Fall | Ankle, neck | RF | 67.0 |
| ADL | Wrist | MLP | 86.0 |
| Pick up | Ankle | LSTM | 18.9 |

Table 2 Comparisons of methods for falls

| Method | Method | Diff of Means | t | $p < 0.05$ |
|---------|---------|---------------|------|------------|
| LSTM | MLP | 0.081 | 9.02 | Yes |
| LSTM | XGBoost | 0.035 | 3.91 | Yes |
| LSTM | RF | 0.008 | 0.87 | No |
| RF | MLP | 0.07 | 8.15 | Yes |
| RF | XGBoost | 0.03 | 3.04 | Yes |
| XGBoost | MLP | 0.05 | 5.11 | Yes |

Table 3 Comparisons of body regions for falls

| Region | Region | Diff of means | t | $p < 0.05$ |
|--------------|--------------|---------------|------|-------------|
| Neck | Wrist | 0.22 | 7.61 | Yes |
| Neck | Belt | 0.086 | 2.95 | Yes |
| Neck | Right pocket | 0.055 | 1.87 | No |
| Neck | Ankle | 0.005 | 0.16 | Do not test |
| Ankle | Wrist | 0.22 | 7.44 | Yes |
| Ankle | Belt | 0.08 | 2.78 | No |
| Ankle | Right pocket | 0.05 | 1.71 | Do not test |
| Right pocket | Wrist | 0.17 | 5.73 | Yes |
| Right pocket | Belt | 0.03 | 1.07 | Do not test |
| Belt | Wrist | 0.14 | 4.66 | Yes |

($t < 0.001$) and XGBoost ($t = 0.002$) methods while RF was greater than MLP ($t < 0.001$) and XGBoost ($t = 0.024$) and XGBoost was greater than MLP ($t < 0.001$). For ADL, MLP method was statistically greater than LSTM ($t < 0.001$) and RF ($t < 0.001$) methods while RF and XGBoost were greater than LSTM ($t < 0.001$). In terms of body regions, neck was statistically greater than belt ($t < 0.001$) and right pocket ($t = 0.005$), while wrist was greater than belt ($t < 0.001$) and right pocket ($t = 0.008$) and ankle was greater than belt ($t = 0.018$). For pick-up, the LSTM method was statistically greater than RF, XGBoost, and MLP ($t < 0.001$).

3.2 Perceived Comfort Analysis

According to [25] the design of a wearable body sensor system attempts to optimize quantitative design parameters (size, weight, battery lifetime, functionality, performance) as well as qualitative design measures, as comfort and social acceptability. Authors consider the comfort level of wearables depends on the number of components and the on-body local-

Table 4 General performance of methods considering sensors positioned in each body region

| Region | Method | Model accuracy |
|--------------|---------|----------------|
| Ankle | RF | 67.0 |
| Ankle | MLP | 70.7 |
| Ankle | XGBoost | 69.8 |
| Ankle | LSTM | 59.4 |
| Waist | RF | 54.4 |
| Waist | MLP | 58.8 |
| Waist | XGBoost | 56.1 |
| Waist | LSTM | 45.7 |
| Neck | RF | 74.8 |
| Neck | MLP | 78.2 |
| Neck | XGBoost | 78.7 |
| Neck | LSTM | 57.7 |
| Right pocket | RF | 61.9 |
| Right pocket | MLP | 70.5 |
| Right pocket | XGBoost | 62.5 |
| Right pocket | LSTM | 52.7 |
| Wrist | RF | 71.3 |
| Wrist | MLP | 75.9 |
| Wrist | XGBoost | 73.6 |
| Wrist | LSTM | 65.8 |

ization. To enhance the wearables' comfort, the number of worn sensors should be reduced, even if increasing the number of wearables can improve reliability. A questionnaire to measure wearables' comfort was proposed in [24]. They assessed perceived comfort along three dimensions: acceptability in terms of looks, anxiety about being monitored, and attachment. A study presented in [26] analyzed the overall comfort of wearables for several body regions including hip, ankle, wrist, abdomen, and shoulder (near to neck). They proposed an approach to rank the body locations to attach the sensors, ordered from the most comfortable to the least comfortable. The aforementioned studies were analyzed and we proposed to map the model of [26] to perceived comfort dimensions in [24] in the following way: Social Acceptability to Acceptability axis; Proxemics, Pressure Pain Threshold, and Motion Impedance to Anxiety; Touch Sensitivity, Pain Sensitivity and Tissue Volume to Attachment. For all three dimensions of the [24], values from [26] less than 0.5 were classified as low level, values from 0.5 to 0.7 were classified as medium and values above 0.7 were considered high level. Higher values of acceptability and lower values of anxiety and attachment represent more comfortable on-body locations. We summarized our approach of the perceived comfort in Table 5, considering one wearable device attached to the body and activities for a day in free-living conditions.

4 Discussion

The hypothesis of the research was supported by the study findings. LSTM or RF algorithms associated with a wearable device, coupled with accelerometers and gyroscopes, positioned

Table 5 Perceived comfort for body regions

| Body region | Acceptability | Anxiety | Attachment |
|--------------|---------------|---------|------------|
| Ankle | High | Low | High |
| Waist (belt) | High | Medium | Medium |
| Neck | High | Low | Medium |
| Hip | Low | High | High |
| Wrist | High | Low | Medium |

at neck or ankle have been found out to reduce both false positive and false negative fall detections while improving fall detection accuracy. According to Table 1 none of the five regions analyzed was the best to correctly classify the 03 classes of activities and no algorithm was the best for all activities. The analysis of confusion matrices in Figs. 6 and 7 showed that the neck region presented the greater positive fall detections while Fig. 8 showed ankle and Fig. 5 found ankle and neck as greater for positive fall detections. Confusion matrices provided accuracy values from 39% to 67% for Fall while values in the range of 56% to 86% for ADL. It was observed that none of the combinations of region and algorithm was able to correctly classify the activity “Pick up an object”, however, most of the rounds classified pick up as ADL. According to Table 4, XGBoost combined with neck had the best outcomes of average accuracy (78.7%). Despite this, RF and neck classified falls better with a hit rate of 67%. Moreover, RF and LSTM methods were statistically greater than MLP and XGBoost for fall detection (Table 2). For fall detection, considering only one wearable sensor (accelerometer and gyroscope data), we pointed out the LSTM deep learning and RF methods were the best machine learning. LSTM was statistically greater than MLP and XGBoost, achieving an accuracy of 60%. No significant difference was found between LSTM and RF. A suitable number of worn-sensors combined with comfortable on-body locations depict a trade-off between functionality and comfort. Table 5 shown neck and wrist as high acceptability, low anxiety, and medium attachment, meaning wearables more comfortable.

According to [3], approaches of deep learning are becoming the state-of-the-art for fall detection. On the other hand, [14] achieved 99,99% of accuracy using XGBoost algorithm for data acquired of sensors positioned into five body regions of a multimodal model combining images and accelerometer. [13] performed seven experiments with the same up-fall detection dataset of our study, for different combinations of data and machine learning models, using 70% of the dataset for training and 30% for testing. They reached 70.31% on F1-score analysis and 95.76% of accuracy for MLP from wearable inertial measurement units, while our experiments showed a lower accuracy of 67% in RF and LSTM methods for fall detection. However, we used data provided from only one sensor while [13] used data from all five different wearable sensors (wrist, neck, pocket, waist and ankle). Nevertheless, an amount of improvements should be achieved to increase accuracy of our approach.

While [3] pointed to be a trend adoption of sensor fusion to provide a more robust approach for the detection of elderly falls, [11] and [12] discussed the concerns about the acceptance of wearables by elderly. This manuscript aims to ensure the output value (accuracy) is as optimal as possible to the greater acceptance of the wearables by elderly. For this, our approach explored different pairwise of an only wearable combined to machine learning algorithms, in order to identify the greater combinations for improving comfort and accuracy. Our outcomes showed that the combination of an only wearable device with accelerometer and gyroscope, coupled to the neck with LSTM or RF algorithms obtained the greater accuracy and comfort among evaluated experiments.

Transformers Neural Models (TNM) [28] have been widely used recently. However, transformers do not process data sequentially in its original form. Instead, it processes the entire data stream. Nevertheless, there are new strategies in the literature so that the TNM can also be used in time series forecasting [29]. In future work, we can use Transformers to increase the generalization of our model.

5 Limitations

Some limitations of the study need to be addressed. We used a public dataset, where falls were simulated by young healthy subjects. However, our study is aimed to elderly. A benchmark dataset to evaluate and compare elderly fall detection systems is still a open challenge. According to [3] the non-linear fusion of multiple sensors is a current trend of elderly fall detection and prediction, which can be hit by machine learning approaches. Nevertheless, our experiments were limited to only a single sensor, positioned on one part of the body. No experiments were performed combining 2 or more wearable sensors.

6 Conclusions

This study seeks to identify, from five human body regions commonly used to wear the wearables, which one would be the most accurate for a real-time falling detector. The on-body regions investigated were: wrist, neck, hip (right pocket), mid-waist (belt), and ankle. Data from the accelerometer and gyroscope were analyzed since they are feasible to incorporate into wearable devices. Previous studies have reported difficulties to distinguish the activity of picking up from falling activities. For this, we gathered up the eleven activities into three classes: Fall, Pick up, and ADL. Experiments carried out evidenced the difficulty that classifiers have to differentiate picking up in particular from the others. Based on the evaluation metrics, the body regions with the most accuracy to differentiate falling and daily activities were neck and ankle. These body regions were statistically greater than the wrist and belt. The wrist was one of the on-body locations with the worst general performance. Since the machine learning algorithms misclassified about 30% of the falls, this study suggests a new investigation of two or more on-body regions to attach wearable sensors or using feature generation techniques. Considering accuracy and comfort, this study suggests to attach comfortable wearable to neck combined to Random Forest or LSTM methods, for real-time detection falls. Nevertheless, combinations of two or more worn-sensors attached to body should be evaluated on providing reliability, choosing the wearables from the most to the least comfortable.

Funding This study was funded by research Project Socio enativos from FAPESP [Grant # 2015/165280].

Data Availability A publicly available multimodal dataset “Up-fall detection dataset” available in <http://sites.google.com/up.edu.mx/har-up/>, according to [13].

Declarations

Conflict of interest The authors declare that they have no conflict of interest.

References

- Sherrington C, Fairhall N, Wallbank G, Tiedemann A, Michaleff Z, Howard K, Clemson L, Hopewell S, Lamb S (2019) Exercise for preventing falls in older people living in the community. *Cochrane Database Syst Rev*. <https://doi.org/10.1002/14651858.cd012424.pub2>
- Saftari LN, Kwon O-S (2018) Ageing vision and falls: a review. *J Physiol Anthropol*. <https://doi.org/10.1186/s40101-018-0170-1>
- Wang X, Ellul J, Azzopardi G (2020) Elderly fall detection systems: a literature survey. *Front Robot AI* 7:71. <https://doi.org/10.3389/frobt.2020.00071>
- Villar JR, Chira C, de la Cal E, González VM, Sedano J, Khojasteh SB (2020) Autonomous on-wrist acceleration-based fall detection systems: unsolved challenges. *Neurocomputing*. <https://doi.org/10.1016/j.neucom.2019.12.147>
- Ozcan K, Velipasalar S, Varshney PK (2017) Autonomous fall detection with wearable cameras by using relative entropy distance measure. *IEEE Trans Hum Mach Syst* 47(1):31–39. <https://doi.org/10.1109/THMS.2016.2620904>
- Li X, Nie L, Xu H, Wang X (2018) Collaborative fall detection using smart phone and Kinect. *Mob Netw Appl* 23(4):775–788. <https://doi.org/10.1007/s11036-018-0998-y>
- Khan AH, Cao X, Li S, Katsikis VN, Liao L (2020) BAS-ADAM: an ADAM based approach to improve the performance of beetle antennae search optimizer. *IEEE/CAA J Automatica Sinica* 7(2):461–471. <https://doi.org/10.1109/JAS.2020.1003048>
- Khan AH, Cao X, Katsikis VN, Stanimirović P, Brajević I, Li S, Kadry S, Nam Y (2020) Optimal portfolio management for engineering problems using nonconvex cardinality constraint: a computing perspective. *IEEE Access* 8:57437–57450. <https://doi.org/10.1109/ACCESS.2020.2982195>
- Abadi I, Zainudin A, Imron C, Fitriyanah DN (2019) Artificial intelligent based fall detection system for elderly people using IoT. In: 2019 International conference on advanced mechatronics, intelligent manufacture and industrial automation (ICAMIMIA), pp 19–24. <https://doi.org/10.1109/ICAMIMIA47173.2019.9223419>
- Khan AH, Li S, Luo X (2020) Obstacle avoidance and tracking control of redundant robotic manipulator: an RNN-based metaheuristic approach. *IEEE Trans Ind Inform* 16(7):4670–4680. <https://doi.org/10.1109/TII.2019.2941916>
- Li H, Wu J, Gao Y, Shi Y (2016) Examining individuals' adoption of healthcare wearable devices: an empirical study from privacy calculus perspective. *Comput Methods Progr Biomed*. <https://doi.org/10.1016/j.ijmedinf.2015.12.010>
- Peek S, Wouters E, Hoof J, Luijckx K, Boeije H, Vrijhoef H (2014) Factors influencing acceptance of technology for aging in place: a systematic review. *Int J Med Inform*. <https://doi.org/10.1016/j.ijmedinf.2014.01.004>
- Martínez-Villaseñor L, Ponce H, Brieva J, Moya-Albor E, Nuñez Martínez J, Peñafort-Asturiano C (2019) Up-fall detection dataset: a multimodal approach. *Sensors* 19:1988. <https://doi.org/10.3390/s19091988>
- Chen T, Guestrin C (2016) XGBoost: a scalable tree boosting system. In: *Proceedings of the 22nd ACM SIGKDD international conference on knowledge discovery and data mining*, pp 785–794
- Tin Kam Ho (1998) The random subspace method for constructing decision forests. *IEEE Trans Pattern Anal Mach Intell* 20(8):832–844
- Kocyyigit Y, Alkan A, Erol H (2008) Classification of EEG recordings by using fast independent component analysis and artificial neural network. *J Med Syst* 32(1):17–20
- McClelland JL, Rumelhart DE, Group PR et al. (1986) Parallel distributed processing. *Explor Microstruct Cogn* 2:216–271
- Breiman L (1999) Random forests—random features. Technical Report vol 567, University of California, Berkeley CA, USA
- Lindner C, Bromiley PA, Ionita MC, Cootes TF (2015) Robust and accurate shape model matching using random forest regression-voting. *IEEE Trans Pattern Anal Mach Intell* 37(9):1862–1874. <https://doi.org/10.1109/TPAMI.2014.2382106>
- Meyer BM, Tulipani LJ, Gurchiek RD, Allen DA, Adamowicz L, Larie D, Solomon AJ, Cheney N, McGinnis R (2020) Wearables and deep learning classify fall risk from gait in multiple sclerosis. *IEEE J Biomed Health Inform*. <https://doi.org/10.1109/JBHI.2020.3025049>
- Sak H, Senior A, Beaufays F (2014) Long short-term memory based recurrent neural network architectures for large vocabulary speech recognition. *arXiv preprint arXiv:1402.1128*
- Tunca C, Salur G, Ersoy C (2020) Deep learning for fall risk assessment with inertial sensors: utilizing domain knowledge in spatio-temporal gait parameters. *IEEE J Biomed Health Inform* 24(7):1994–2005. <https://doi.org/10.1109/JBHI.2019.2958879>

23. Wen J, Yang Z, Jin L (2020) Wireless signal based elderly fall detection using XGBoost algorithm. In: 2020 IEEE international conference on smart internet of things (SmartIoT), pp 304–308. <https://doi.org/10.1109/SmartIoT49966.2020.00054>
24. Hegde N, Bries M, Swibas T, Melanson E, Sazonov E (2018) Automatic recognition of activities of daily living utilizing insole-based and wrist-worn wearable sensors. *IEEE J Biomed Health Inform* 22(4):979–988. <https://doi.org/10.1109/JBHI.2017.2734803>
25. Falch L, de Silva CW (2018) An approach to optimize multiple design objectives with qualitative and quantitative criteria for a wearable body sensor system. *IEEE Sens J* 18(23):9708–9717. <https://doi.org/10.1109/JSEN.2018.2871676>
26. Falch L, de Silva C (2020) Incorporating the qualitative variable comfort into the design of a wearable body sensor system. *IEEE/ASME Trans Mechatron*. <https://doi.org/10.1109/TMECH.2020.3004190>
27. Kingma DP, Ba J (2014) ADAM: a method for stochastic optimization. arXiv preprint [arXiv:1412.6980](https://arxiv.org/abs/1412.6980)
28. Vaswani A, Shazeer N, Parmar N, Uszkoreit J, Jones L, Gomez AN, Kaiser L, Polosukhin I (2017) Attention is all you need. In: Guyon I, Luxburg UV, Bengio S, Wallach H, Fergus R, Vishwanathan S, Garnett R (eds) *Advances in neural information processing systems*, vol 30, Curran Associates, Inc., pp 5998–6008
29. Lim B, Arık SÖ, Loeff N, Pfister T (2021) Temporal fusion transformers for interpretable multi-horizon time series forecasting. *Int J Forecast* 37(4):1748–1764. <https://doi.org/10.1016/j.ijforecast.2021.03.012>

Publisher's Note Springer Nature remains neutral with regard to jurisdictional claims in published maps and institutional affiliations.